Thermodynamic View of Primary Gushing

Sylvie M. Deckers,[1,2] Lennert Vissers,[1] Mohammadreza Khalesi,[1] Zahra Shokribousjein, Hubert Verachtert, and Kurt Gebruers, *KU Leuven, Department of Microbial and Molecular Systems (M²S), Leuven Food Science and Nutrition Research Centre (LFoRCe) and Leuven Institute for Beer Research (LIBR), BE-3001 Heverlee, Belgium;* **Xavier Pirlot,** *Chimay Brewery, BE-6464 Baileux, Belgium;* **Jean-Marie Rock,** *Orval Brewery, BE-6823, Villers-devant-Orval, Belgium;* **Vladimir Ilberg,** *Hochschule Weihenstephan-Triesdorf, Fakultät Gartenbau and Lebensmitteltechnologie, D-85350 Freisinig, Germany;* **Jean Titze,** *National University of Ireland, University College Cork, School of Food and Nutritional Sciences, Cork, Ireland;* **Hedwig Neven,** *KU Leuven, Department of Microbial and Molecular Systems (M²S), Leuven Food Science and Nutrition Research Centre (LFoRCe) and Leuven Institute for Beer Research (LIBR), BE-3001 Heverlee, Belgium; and Brewery Duvel-Moortgat, BE-2870 Puurs, Belgium;* **and Guy Derdelinckx,** *KU Leuven, Department of Microbial and Molecular Systems (M²S), Leuven Food Science and Nutrition Research Centre (LFoRCe) and Leuven Institute for Beer Research (LIBR), BE-3001 Heverlee, Belgium*

ABSTRACT

J. Am. Soc. Brew. Chem. 71(3):149-152, 2013

A spontaneous, wild, and uncontrolled liquid expulsion immediately upon opening non-shaken bottles of carbonated beverages defines primary gushing. The liquid volume resulting from primary gushing differs greatly even in the same laboratory. A thermodynamic investigation of the process can determine parameters responsible for this phenomenon. Although the required energy to provoke gushing is believed to be obtained mostly by the expansion of the nanobubbles, there are many other sources that might be significantly involved in this case. Providing the required energy via the explosion of the nanobombs breaks the weak hydrogen bond between CO_2 and water molecules and results in the release of the CO_2. In this study, the authors claim that primary gushing is mainly linked to the CO_2 properties and consequently related to the liquid temperature at bottle opening (K), the pressure (bar), the CO_2 concentration (g/L), and the energy (N.m).

Keywords: Carbon dioxide, Hydrogen bond, Hydrophobin, Primary gushing, Thermodynamics

RESUMEN

A la expulsión de líquido espontánea, salvaje y descontrolada inmediatamente después de la apertura de botellas de bebidas carbonatadas sin agitación define el gushing principal. El volumen de líquido que resulta de gushing principal es muy diferente, incluso en el mismo laboratorio. Una investigación termodinámica del proceso puede determinar los parámetros responsables de este fenómeno. Aunque se cree que la energía requerida para provocar gushing a ser obtenido principalmente por la expansión de los nanoburbujas, hay muchas otras fuentes que pudieran estar implicados significativamente en este caso. Proporcionar la energía necesaria a través de la explosión de la nanobombs rompe el enlace de hidrógeno débiles entre las moléculas de CO_2 y agua y resulta en la liberación del CO_2. En este estudio, los autores afirman que gushing principal está vinculada principalmente a las propiedades de CO_2 y, por consiguiente relacionada con la temperatura del líquido en la abertura de la botella (K), la presión (bar), la concentración de CO_2 (g/L), y la energía (nm).

Palabras claves: Dióxido de carbono, Enlace de hidrógeno, Gushing principal, Hidrofobina, Termodinámica

[1] These authors contributed equally to the work.

[2] Corresponding author. E-mail: Sylvie.Deckers@biw.kuleuven.be; phone: +32-16-328535; fax: +32-16-321997

INTRODUCTION

In order to obtain the gushing potential of malt or beer wort, a reasonable amount of malt extract or wort sample is usually supplemented to a carbonated beverage such as sparkling water or non-gushing beer (7,15). However, the problem with this common method is that the volume of the liquid expelled from a test bottle is greatly dependent on the internal and external variations (13). The structure of hydrophobin present in the bottle (14), the CO_2 concentration, and the type of beverage test (13,15), as well as the extract preparation method (4) influence the gushing volume. Beside the Class II hydrophobins, it is hypothesized that gushing occurs when the barley grain ns-LTP1 level exceeds a threshold value (9). However, Hippeli and Hecht (11) detected lower amount of ns-LTP1 in bottles of gushing beer than in non-gushing beer of the same brand (11,12). Also, it was shown that ns-LTPs were not gushing inducers (12,16), but in contrast, were able to reduce the gushing volume induced by Class II hydrophobins (12). Based on the well described mechanism (6), primary gushing is therefore induced by CO_2 bubbles stabilized at a critical diameter (depending on the pressure inside the closed bottle) as a consequence of the self-assembly of class II hydrophobin.

Sarlin et al (14) reported that only 3 µg/L of class II hydrophobin produced by *Trichoderma reesei* is sufficient to induce primary gushing and therefore, the quantity of nanobubbles is limited by the class II hydrophobin concentration. Later, Christian et al (3) found a relation between the overfoaming volume and the shaking duration of the bottles. The agitation (i.e., supplemented energy) was therefore considered as a significant parameter responsible for the nanobubble quantity. Also it is observed that the gushing volume is greatly affected by the temperature of the beverage at bottle opening (Fig. 1). The level of carbonation is another issue for the gushing volume.

Although the most effective factors for gushing amount have been discussed in previous studies (8,13), the thermodynamic properties of those parameters are still a missing part of this phenomenon. Hence, in this study, the authors attempt to make the principle of gushing more clear in the view of thermodynamics.

THEORETICAL CALCULATION

Number of CO_2 Molecules in a Stabilized Nanobubble

To determine the critical diameter of the CO_2 bubbles at 4 bar pressure, equation 1 (Boyle Mariotte's law) for the ideal gas law is used.

$$P_{1bar} \times V_{1bar} = \text{constant}$$
$$P_{1bar} \times V_{1bar} = P_{4bar} \times V_{4bar} \tag{1}$$

Fig. 1. The visual effect of beverage temperature on the gushing volume. Left, at 2°C only 10 g are expelled from a 330 mL bottle and right, at 25°C, 132 g are expelled from a 330 mL bottle of the same brand.

where P_{1bar} and P_{4bar} represent the pressure at 1 and 4 bar, respectively, and V_{1bar} and V_{4bar} indicate the volume of CO_2 bubbles at 1 and 4 bar, respectively. The critical diameter of the CO_2 bubbles at atmospheric pressure was reported to be 100 nm (5,6). The calculated volume of the nanobubble ($V = 4\pi r^3/3$) at 1 bar is therefore 5.24×10^5 nm^3. It is then possible to determine its critical diameter at 4 bar by Boyle Mariotte's law. Considering equation 1, the volume of the CO_2 bubble at 4 bar pressure is calculated as below:

$$V_{4bar} = \frac{P_{1bar} \times V_{1bar}}{P_{4bar}} = \frac{1 \, bar \times 5.24 \times 10^5 \, nm^3}{4 \, bar} = 1.31 \times 10^5 \, nm^3 \quad (2)$$

and therefore, the critical diameter (d_{4bar}) of the CO_2 nanobubble at 4 bar is obtained as below:

$$r_{4bar} = \sqrt[3]{\frac{3V_{4bar}}{4\pi}} = \sqrt[3]{\frac{3 \times 1.31 \times 10^5 \, nm^3}{4\pi}} = 31.5 \, nm$$

$$d_{4bar} = 63 \, nm \quad (3)$$

The volume of one CO_2 molecule (V_{CO2}) was estimated to be 0.033 nm^3 using the van der Waals volume. We assume that the CO_2 bubble at 4 bar is totally occupied by the molecule of CO_2 without any free space or any overlapping between molecules. The number of CO_2 molecules in one bubble is therefore estimated to be as the following:

$$\frac{V_{4bar}}{V_{CO2}} = \frac{1.31 \times 10^5 \, nm^3}{0.033 \, nm^3} = 3.9 \times 10^6 \, molecules \quad (4)$$

Thermodynamic Properties of Gushing

The gushing phenomenon follows the first law of thermodynamics since there is not any thermal transfer. Hence, it takes place at adiabatic conditions. Furthermore, the system is considered as the atmospheric environment, because first of all, this is a closed system where the changes are negligible and secondly, this system occurs at low pressure (4 bar). Thus, the equation of Avogadro (equation 5), which is applicable only for ideal gases, can be used:

$$PV = nRT \quad (5)$$

where P is the pressure (Pa or N/m^2), V is the volume occupied by the gas (m^3), n is the quantity of matter (mol), R is the universal constant of ideal gas (8.31 J/Kmol), and T is the temperature (K).

Because 1 mole of CO_2 contains 6.022×10^{23} molecules (Avogadro's number), the quantity of matter present in one bubble is therefore determined:

$$n = \frac{3.9 \times 10^6 \, molecules}{6.022 \times 10^{23} \, molecules \, per \, mol} = 6.64 \times 10^{-18} \, mol \quad (6)$$

The energy (E) content in a bubble with a diameter of 63 nm at 25°C (i.e., 298 K) is determined by the equation of Avogadro:

$$PV = nRT = 6.64 \times 10^{-18} \, mol \times 8.31 \, J/Kmol \times 298 \, K$$
$$= 1.63 \times 10^{-14} \, J/bubble \quad (7)$$

In order to expel 200 mL (~200 g) of the liquid up to 15 cm height at 25°C, the nanobubbles deliver the required energy for expulsion by relaxation during depressurization (Equation 8).

$$Work = energy \times pressure = \left(\frac{kg}{ms^2}\right) \times m^3 = \frac{kg \times m^2}{s^2} = J$$

Work needed to expel 200 mL (0.2 kg) up to 15 cm (0.15 m)

$$height \, in \, 1 \, second = 0.2 \, kg \times \frac{(15 \times 10^{-2} \, m)^2}{1^2 s^2} = 4.5 \times 10^{-3} \, J \quad (8)$$

Combining the equations 7 and 8, the number of nanobubbles is determined as follows:

$$Number \, of \, bubbles =$$
$$\frac{Work \, needed \, to \, expel \, 200 \, mL \, up \, to \, 15 \, cm \, height \, in \, 1 \, second}{Energy \, in \, one \, bubble} =$$
$$\frac{4.5 \times 10^{-3} \, J}{1.63 \times 10^{-14} \, J/bubble} = 2.76 \times 10^{11} \, bubbles \quad (9)$$

The surface of one nanobubble ($4\pi r^2$) is 1.2469×10^4 nm^2. In addition, the solvent accessible area of the hydrophobic patch of hydrophobin HFBII was reported to be 7.4 nm^2 (10). Besides, it should be noted that only 2/3 of the bubble surface is considered to be covered by hydrophobin due to overlapping of molecules. Considering the latter, the amount of hydrophobin monomers and the mass of hydrophobin that totally covers the surface of one bubble is calculated as below:

$$Amount \, of \, monomer \, of \, HFBII \, covering \, one \, bubble =$$
$$\frac{2}{3} \times \frac{S_{4bar}}{S_{patch}} = \frac{2}{3} \times \frac{12,469 \, nm^2}{7.4 \, nm^2} = 1,123 \, monomers \quad (10)$$

$$Mass \, of \, \frac{HFBII}{bubble} = 7.2 \times 10^3 \, Da \times 1.66 \times 10^{-18} \, \frac{\mu g}{Da}$$
$$\times 1,123 \, monomers = 1.34 \times 10^{-11} \, \frac{\mu g}{bubble} \quad (11)$$

Consequently, the amount of hydrophobin needed to expel 200 mL up to 15 cm height is determined as follows and corresponds to 4 μg:

$$Amount \, of \, hydrophobin \, needed \, to \, expel \, 200 \, mL =$$
$$2.76 \times 10^{11} \, bubbles \times 1.34 \times 10^{-11} \, \frac{\mu g}{bubble} = 3.7 \, \mu g \quad (12)$$

Interestingly, after some experiments in 2005, Sarlin et al (14) reported that only 10 μg/330 mL of *T. reesei* HFBII is sufficient to induce an overfoaming of 200 mL. However, our calculation indicate that only 3.7 μg would be enough to expel 200 mL. But we did not take into account that the height to expel the liquid varies during the overfoaming. The more the bottle is filled out, the

Fig. 2. Hydrogen bonds (grey bar) formed between different water molecules (1).

Fig. 3. The CO_2-water cluster. The oxygen atoms are shown in black, the hydrogen atoms are shown in light gray, and the carbon atom is shown in dark gray with white dots (2).

more the height to expel the liquid increases, resulting in a higher energy requiring more nanobubbles and hydrophobins. The amount of hydrophobins obtained is then underestimated. If we take into account the variation in the height, the amount of needed hydrophobins would be higher than 10 μg observed in practice. Moreover, our calculations are valid only if all the energy comes from nanobubbles and if the 200 mL are expelled at 15 cm height. In practice, the height is much higher than 15 cm, which means that extra energy needs to be liberated.
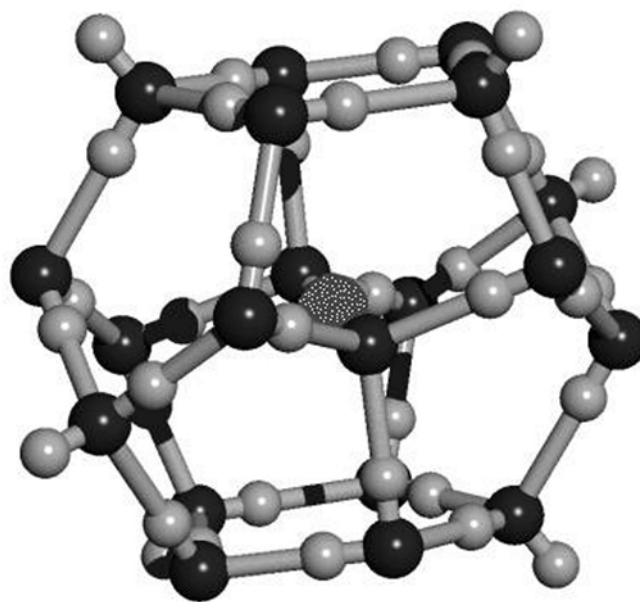
The Effect of Bottle Opening Temperature on the Thermodynamic Properties

If the same bottle, as mentioned above, is opened at 2°C (275 K), the same amount of energy may expel 187 mL of the liquid instead of 200 mL at 25°C:

$$\text{Energy liberated by } 2.76 \times 10^{11} \text{ bubbles if the bottle is opened at } 2°C = 6.64 \times 10^{-18} \text{ mol} \times 8.31 \text{ J/Kmol} \times 275 \text{ K} \times 2.76 \times 10^{11} \text{ bubbles} = 4.2 \times 10^{-3} \text{ J} \quad (13)$$

Practically, a much higher volume is expelled at 25°C (132 g) in comparison with 2°C (10 g). This difference is explained by the binding and the solubility of the gas, which depends importantly on the temperature and also by the nanobomb effect. The binding and the solubility is higher at chilling temperature (2°C) than at room temperature (25°C). Considering the nanobomb theory reported by Deckers et al (5,6), it is assumed that at the bottle opening, the depressurization results in explosion of the nanobubbles stabilized by hydrophobins. This explosion releases an initial amount of mechanical energy, under the form of vibrations or shaking energy in the liquid, which is responsible for breaking of the weak bond (i.e., hydrogen bond [Fig. 2] [1]) between CO_2 and liquid. As explained in our previous study (6), CO_2 in carbonated beverages is present in the dissolved form ($CO_{2(aq)}$) and not in the carbonic acid form (H_2CO_3). In fact, the oxygen atoms in CO_2 can make specific hydrogen bonding with water molecules (2). The CO_2 may form a hydration shell from a symmetrical dodecahedral arrangement of 18 water molecules where each CO_2 oxygen atom is bonded to three water molecules (Fig. 3) (2).

By these considerations, it can be proposed that at the bottle opening (i.e., depressurization), the nanobubbles stabilized by class II hydrophobin will explode, resulting in the release of vibration energy (nanobomb effect). The latter is sufficient to break the hydrogen bonds between CO_2 and water. This results in the liberation of CO_2 and gushing by CO_2 diffusion in the nucleation sites formed. The higher the CO_2 concentration is, the greater the gushed liquid is due to the higher pressure (i.e., nanobomb effect). Consequently, the amount of CO_2 that escapes is greater. The effect of the temperature is explained by its influence on the pressure (i.e., nanobomb effect), on the CO_2 solubility, and on the CO_2 binding. At 25°C, after the nanobomb effect, more CO_2 molecules escape due to the lower solubility, and this results in higher overfoaming at 25°C in comparison with the opening at 2°C.

CONCLUSION

At the bottle opening, the pressure drops from 4 to 1 bar, resulting in the expansion of the gas. The crystalline layer formed by the self-assembly of class II hydrophobin around CO_2 bubbles is neither solid nor elastic enough to resist against such a gas expansion. The stabilized nanobubbles explode with a release of energy in the form of vibration energy, which is called the "nanobomb effect." This energy is sufficient to break the weak hydrogen bond between CO_2 and water molecules and is responsible for the CO_2 release. Nevertheless, it is also affected by the type and the concentration of hydrophobin as well as the preparation of the grain extract. This highlights the fact that the overfoaming volume is mainly linked to CO_2 properties! In fact, gushing potential is positively related to the bottle opening temperature, the pressure, the CO_2 concentration, and the released energy.

LITERATURE CITED

1. Byrd, J., and Perona, M. Surface tension and soap bubble. http://wwwchem.csustan.edu/chem2000/Exp5/Bkg.htm, accessed August 13, 2012.
2. Chaplin, M. Water structure and science, the CO_2-water cluster. http://www.lsbu.ac.uk/water/co2.html, accessed August 13, 2012.
3. Christian, M., Ilberg, V., Titze, J., Friess, A., Jacob, F., and Parlar, H. Gushing laboratory tests as successful methods for obtaining new cognitions on gushing. *Monatsschr. Brauwiss.* 62:83-89, 2009.
4. Christian, M., Ilberg, V., Titze, J., Aydin, A. A., Jacob, F., and Parlar, H. New cognitions on the gushing phenomenon. *32nd Eur. Brew. Conv. Congr.*, Hamburg, Germany, Poster 9, 2009.

5. Deckers, S. M., Gebruers, K., Baggerman, G., Lorgouilloux, Y., Delcour, J. A., Michiels, C., Derdelinckx, G., Martens, J., and Neven, H. CO_2-hydrophobin structures acting as nanobombs in beer. *Monatsschr. Brauwiss.* 63:54-61, 2010.

6. Deckers, S. M., Venken, T., Khalesi, M., Gebruers, K., Baggerman, G., Lorgouilloux, Y., Shokribousjein, Z., Ilberg, V., Schönberger, C., Titze, J., Verachtert, H., Michiels, C., Neven, H., Delcour, J., Martens, J., Derdelinckx, G., and De Maeyer, M. Combined modeling and biophysical characterization of CO_2 interaction with Class II hydrophobins: new insight in the mechanism behind primary gushing, *J. Am. Soc. Brew. Chem.* 70:249-256, 2012.

7. Garbe, L.-A., Nagel, R., Rauschmann, M., Lamers, M., Ehmer, A., and Tressl, R. Correlation of deoxynivalenol, hydrophobins and gushing. *Proc. Eur. Brew. Conv. Congr.*, Venice, 2007.

8. Gardner, R. J. The mechanism of gushing - a review, *J. Inst. Brew* 79:275-283, 1973.

9. Gorjanovic, S. Barley grain non-specific lipid-transfer proteins (ns-LTPs) in beer production and quality. *J. Inst. Brew.* 113:310-324, 2007.

10. Hakanpaa, J., Szilvay, G. R., Kaljunen, H., Maksimainen, M., Linder, M., and Rouvinen, J. Two crystal structures of *Trichoderma reesei* hydrophobin HFBI—The structure of a protein amphiphile with and without detergent interaction. *Protein Sci.* 15:2129-2140, 2006.

11. Hippeli, S., and Hecht, D. The role of ns-LTP1 and proteases in causing primary gushing. *Brauwelt Int.* 27:30-34, 2009.

12. Lutterschmid, G., Muranyi, M., Stübner, M., Vogel, R. F., and Niessen, L. Heterologous expression of surface-active proteins from barley and filamentous fungi in *Pichia pastoris* and characterization of their contribution in beer gushing. *Int. J. Food Microbiol.* 147:17-25, 2011.

13. Rath, F. Gushing in 2008 – Trialling the "Modified Carlsberg Test". *Brauwelt Int.* 27:26-29, 2009.

14. Sarlin, T., Nakari-Setälä, T., Linder, M., Penttilä, M., and Haikara, A. Fungal hydrophobins as predictors of the gushing activity of malt. *J. Inst. Brew.* 111:105-111, 2005.

15. Sarlin, T., Kivioja, T., Kalkkinen, N., Linder, M. B., and Nakari-Setälä, T. Identification and characterization of gushing-active hydrophobins from *Fusarium graminearum* and related species. *J. Basic Microbiol.* 51:1-11, 2011.

16. Zapf, M. W., Theisen, S., Vogel, R. F., and Niessen, L. Cloning of wheat LTP1500 and two *Fusarium culmorum* hydrophobins in *Saccharomyces cerevisiae* and assessment of their gushing inducing potential in experimental wort fermentation. *J. Inst. Brew.* 112:237-245, 2006.